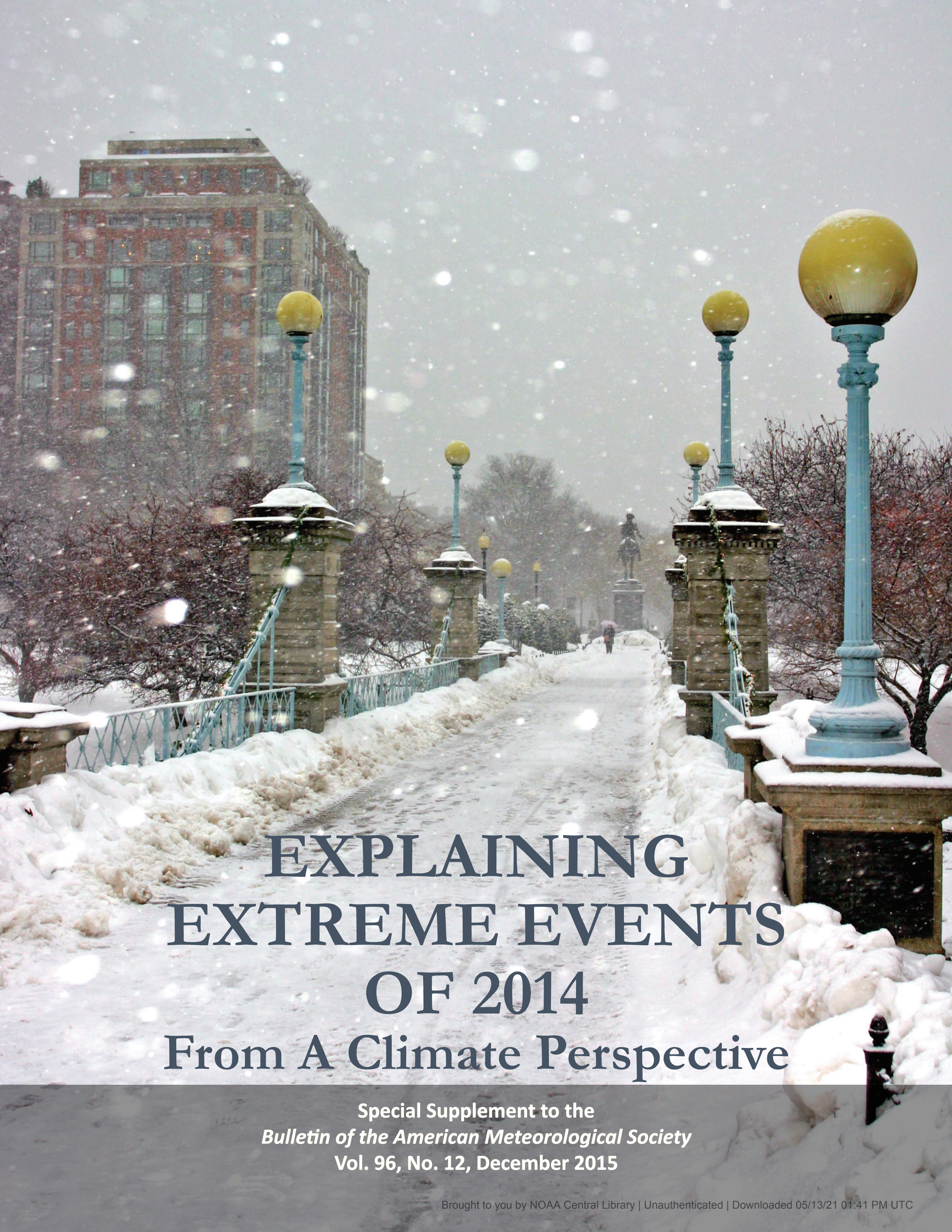

EXPLAINING EXTREME EVENTS OF 2014

From A Climate Perspective

Special Supplement to the
Bulletin of the American Meteorological Society
Vol. 96, No. 12, December 2015

EXPLAINING EXTREME EVENTS OF 2014 FROM A CLIMATE PERSPECTIVE

Editors

Stephanie C. Herring, Martin P. Hoerling, James P. Kossin, Thomas C. Peterson, and Peter A. Stott

Special Supplement to the

Bulletin of the American Meteorological Society

Vol. 96, No. 12, December 2015

AMERICAN METEOROLOGICAL SOCIETY

CORRESPONDING EDITOR:

Stephanie C. Herring, PhD
NOAA National Centers for Environmental Information
325 Broadway, E/CC23, Rm 1B-131
Boulder, CO 80305-3328
E-mail: stephanie.herring@noaa.gov

COVER CREDITS:

FRONT: ©iStockphotos.com/coleong—Winter snow, Boston, Massachusetts, United States.

BACK: ©iStockphotos.com/nathanphoto—Legget, California, United States – August 13, 2014: CAL FIRE helicopter surveys a part of the Lodge Fire, Mendocino County.

HOW TO CITE THIS DOCUMENT

Citing the complete report:

Herring, S. C., M. P. Hoerling, J. P. Kossin, T. C. Peterson, and P. A. Stott, Eds., 2015: Explaining Extreme Events of 2014 from a Climate Perspective. *Bull. Amer. Meteor. Soc.*, **96** (12), S1–S172.

Citing a section (example):

Yoon, J. H., S.-Y. S. Wang, R. R. Gillies, L. Hipps, B. Kravitz, and P. J. Rasch, 2015: Extreme fire season in California: A glimpse into the future? [in "Explaining Extremes of 2014 from a Climate Perspective"]. *Bull. Amer. Meteor. Soc.*, **96** (12), S5–S9.

EDITORIAL AND PRODUCTION TEAM

Riddle, Deborah B., Lead Graphics Production, NOAA/NESDIS National Centers for Environmental Information, Asheville, NC

Love-Brotak, S. Elizabeth, Graphics Support, NOAA/NESDIS National Centers for Environmental Information, Asheville, NC

Veasey, Sara W., Visual Communications Team Lead, NOAA/NESDIS National Centers for Environmental Information, Asheville, NC

Griffin, Jessicca, Graphics Support, Cooperative Institute for Climate and Satellites-NC, North Carolina State University, Asheville, NC

Maycock, Tom, Editorial Support, Cooperative Institute for Climate and Satellites-NC, North Carolina State University, Asheville, NC

Misch, Deborah J., Graphics Support, LMI Consulting, Inc., NOAA/NESDIS National Centers for Environmental Information, Asheville, NC

Osborne, Susan, Editorial Support, LMI Consulting, Inc., NOAA/NESDIS National Centers for Environmental Information, Asheville, NC

Schreck, Carl, Editorial Support, Cooperative Institute for Climate and Satellites-NC, North Carolina State University, and NOAA/NESDIS National Centers for Environmental Information, Asheville, NC

Sprain, Mara, Editorial Support, LAC Group, NOAA/NESDIS National Centers for Environmental Information, Asheville, NC

Young, Teresa, Graphics Support, STG, Inc., NOAA/NESDIS National Centers for Environmental Information, Asheville, NC

TABLE OF CONTENTS

ABSTRACT—Stephanie C. Herring, Martin P. Hoerling, James P. Kossin, Thomas C. Peterson, and Peter A. Stott

Understanding how long-term global change affects the intensity and likelihood of extreme weather events is a frontier science challenge. This fourth edition of explaining extreme events of the previous year (2014) from a climate perspective is the most extensive yet with 33 different research groups exploring the causes of 29 different events that occurred in 2014. A number of this year's studies indicate that human-caused climate change greatly increased the likelihood and intensity for extreme heat waves in 2014 over various regions. For other types of extreme events, such as droughts, heavy rains, and winter storms, a climate change influence was found in some instances and not in others. This year's report also included many different types of extreme events. The tropical cyclones that impacted Hawaii were made more likely due to human-caused climate change. Climate change also decreased the Antarctic sea ice extent in 2014 and increased the strength and likelihood of high sea surface temperatures in both the Atlantic and Pacific Oceans. For western U.S. wildfires, no link to the individual events in 2014 could be detected, but the overall probability of western U.S. wildfires has increased due to human impacts on the climate.

Challenges that attribution assessments face include the often limited observational record and inability of models to reproduce some extreme events well. In general, when attribution assessments fail to find anthropogenic signals this alone does not prove anthropogenic climate change did not influence the event. The failure to find a human fingerprint could be due to insufficient data or poor models and not the absence of anthropogenic effects.

This year researchers also considered other human-caused drivers of extreme events beyond the usual radiative drivers. For example, flooding in the Canadian prairies was found to be more likely because of human land-use changes that affect drainage mechanisms. Similarly, the Jakarta floods may have been compounded by land-use change via urban development and associated land subsidence. These types of mechanical factors re-emphasize the various pathways beyond climate change by which human activity can increase regional risk of extreme events.

6. EXTREME NORTH AMERICA WINTER STORM SEASON OF 2013/14: ROLES OF RADIATIVE FORCING AND THE GLOBAL WARMING HIATUS

Xiaosong Yang, G. A. Vecchi, T. L. Delworth, K. Paffendorf, R. Gudgel, L. Jia, Seth D. Underwood, and F. Zeng

The extreme 2013/14 winter storm season over much of North America was made more likely by the multiyear anomalous tropical Pacific winds associated with the recent global warming hiatus.

Introduction. Over the period December 2013–February 2014, there was a pronounced reduction of extratropical storm (ETS) activity over the North Pacific Ocean and the west coast of the United States of America (USA), and a substantial increase of ETS activity extending from central Canada down to the midwestern USA (Fig. 6.1a). The ETS activity was measured by the standard deviation of filtered 6-hourly sea level pressure in December–February (DJF) using a 24-hour-difference filter (Wallace et al. 1988). A number of large-scale climate factors could have influenced the probability of this extreme year. Natural climate variations, such as the El Niño–Southern Oscillation (ENSO) and the North Atlantic Oscillation (NAO) significantly influence ETS activity over North America (e.g., Yang et al. 2015; Grise et al. 2013). Our assessment of these factors indicates that they were not major players in the 2013/14 case (not shown). In addition, models suggest that radiative forcing changes can influence the surface storm tracks over North America, including a decrease under global warming (Chang et al. 2013). Furthermore, the recent multiyear drying over the western USA has been linked to the global warming hiatus (Delworth et al. 2015), suggesting the recent multiyear tropical Pacific wind changes that have been linked to the global warming hiatus (Kosaka and Xie 2013; England et al. 2014; Delworth et al. 2015) may impact winter ETS extremes over North America.

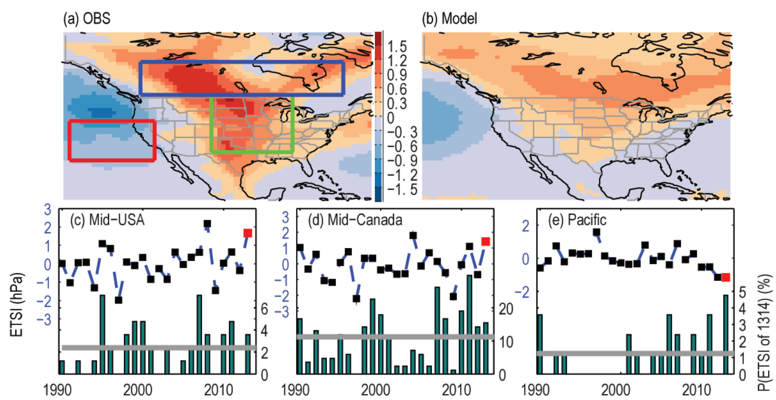

Fig. 6.1. (a) Observed (amplitudes scaled by a factor of 0.5 for displaying) and (b) forecasted ensemble mean ETS anomalies (relative to the 1980–2010 climatology) over North America during 2013/14. The ensemble mean is averaged over 84 members of all available hindcasts starting from 1 November 2013 and 1 December 2013. (c)–(e) Observed ETSI anomalies (dashed with square marker, left y-axis) and the occurrence probability (shaded bar, right y-axis) of the 2013/14 extreme ETSI estimated from the 84-member hindcasts at each year for the mid-USA [green box in (a)], the mid-Canada [blue box in (a)], and the Pacific coastal region [red box in (a)] during 1990–2013. The gray horizontal bar denotes the climatological occurrence probability of the 2013/14 extreme ETSI. Red marker highlights the 2013/14 ETSI.

The ensemble mean of initialized seasonal predictions with a high-resolution coupled model (see next section) predicted the large-scale spatial structure of the observed anomalous ETS in 2013/14 from about

AFFILIATIONS: Yang—NOAA/Geophysical Fluid Dynamics Laboratory, Princeton, New Jersey, and University Corporation for Atmospheric Research, Boulder, Colorado; Vecchi, Delworth, Paffendorf, and Jia—NOAA/Geophysical Fluid Dynamics Laboratory, Princeton, New Jersey, and Atmospheric and Oceanic Sciences Program, Princeton University, Princeton, New Jersey; Gudgel and Zeng—NOAA/Geophysical Fluid Dynamics Laboratory, Princeton, New Jersey; Underwood—Engility Corporation, Chantilly, Virginia

DOI:10.1175/BAMS-D-15-00133.1

A supplement to this article is available online (10.1175/BAMS-D-15-00133.2)

zero to one month ahead, but the predicted amplitudes are much weaker than the observations (Figs. 6.1a,b; Yang et al. 2015). Other studies show that the predicted amplitudes of surface air temperature in 2013/14 winter over North America are also weaker than the observations even given the sea surface temperature (Hartmann 2015). As discussed in Yang et al. (2015), even given climate initialization using the data assimilation, the 2013/14 winter ETS activity over North America was unlikely and thus had a large stochastic ("weather noise" and/or model errors) contribution. However, we can also see that initialization changes the probability of such extreme event from the background probability (Figs. 6.1c–e), indicating there was a climate driver that increased the probability of this extreme event in the 2013/14 season (and in the decade that preceded it). Thus, we here focus on a probabilistic assessment of the extreme ETS event and examine potential climate drivers for it, focusing on radiative forcing changes and the multiyear tropical Pacific wind changes that have been connected to the global warming hiatus. In this study, we use a suite of high-resolution climate model experiments to explore whether the extreme ETS activity over North America in the 2013/14 winter was made more likely by anthropogenic forcing or global warming hiatus.

Methodology. We used the Geophysical Fluid Dynamics Laboratory (GFDL) Forecast-Oriented Low Ocean Resolution model [FLOR; Vecchi et al. 2014; see online supplemental material (SM) Section 1] to conduct a suite of initialized and uninitialized numerical simulations. The observational ETSs were derived from the ERA-Interim reanalysis data during 1979–2014 (Dee et al. 2011). Throughout this study, we select three regions of interest in North America and the Pacific coastal ocean (Fig. 6.1a). Two regions with extremely active ETSs are the mid-USA and mid-Canada, while one region with extremely low ETS activities is California and its surrounding Pacific coastal ocean, hereafter Pacific coastal. The ETS index (ETSI) is formed by an average over each region. Following Murakami et al. (2015), we used a probabilistic rather than a deterministic approach. We will examine the probability of the ETSI of the three regions during DJF as a function of ETSI using the following equation:

$$P(x) = \frac{Number\ of\ years\ with\ ETSI \geq x}{Total\ number\ of\ years} \qquad (1)$$

where x is the ETSI value for a given region. For example, P(ETSI of 2013/14) represents the probability of occurrence of a year with ETSI values equal to or more than that of 2013/14 winter. Note that the Pacific coastal region is in the negative extreme category, so we compute 1–P(ETSI of 2013/14).

The interannual variations of the observed ETSI anomalies over the three regions are shown in Figs. 6.1c–e. The observed ETSI anomalies for 2013/14 are all in the extreme category with climatological empirical occurrence probability values of ~1.5%, ~3%, and ~10% for Pacific coastal, mid-USA, and mid-Canada, respectively. We first examined the retrospective seasonal forecasts made using FLOR for the period 1990–2014 (Vecchi et al. 2014; Jia et al. 2015). To estimate the extreme probability, we combined all available hindcasts of 0–1 month ahead to produce 84 samples for each predicted year (see SM Section 2a). The model predictions provide reliable estimates of the event probabilities (see SM Section 3).

Figures 6.1c–e show the time series of P(ETSI of 2013/14) over the three regions as predicted by FLOR. When compared with the observed ETSI, FLOR reasonably predicted the observed interannual variations, for example, higher (lower) probabilities in line with positive (negative) ETSI anomalies over the mid-USA (correlation coefficient 0.55) and Canada (correlation coefficient 0.47), and vice versa for the negative extreme over the Pacific coast (correlation coefficient −0.41), consistent with the examination of deterministic skill in ETS prediction by Yang et al. (2015). For the year 2013/14, FLOR predicted consistently higher occurrence probability than the climatological probability values over the three regions, indicating the initial conditions played roles in the extreme ETS activity of the 2013/14 winter event.

Effect of anthropogenic forcing and recent global warming hiatus. We generated multicentennial control climate simulations by prescribing radiative forcing and land-use conditions representative of the years 1860 and 1990, and 35-member ensemble simulations with prescribed time-varying historical and projected radiative forcings (see SM Sections 2b and 2c) from 1941 to 2040. The effect of anthropogenic forcing can be estimated by taking the difference of those simulations. Figures 6.2a–c show the extreme occurrence probabilities for the three regions respectively. The probabilities estimated from the 1860 and 1990 control experiments are not statistically distinguishable for any of the three regions (first column of Figs. 6.2a–c). There is no statistically significant change of the extreme occurrence probabilities over mid-USA during 1940–2040 (second column of Fig. 6.2a); the extreme occurrence probabilities over mid-Canada

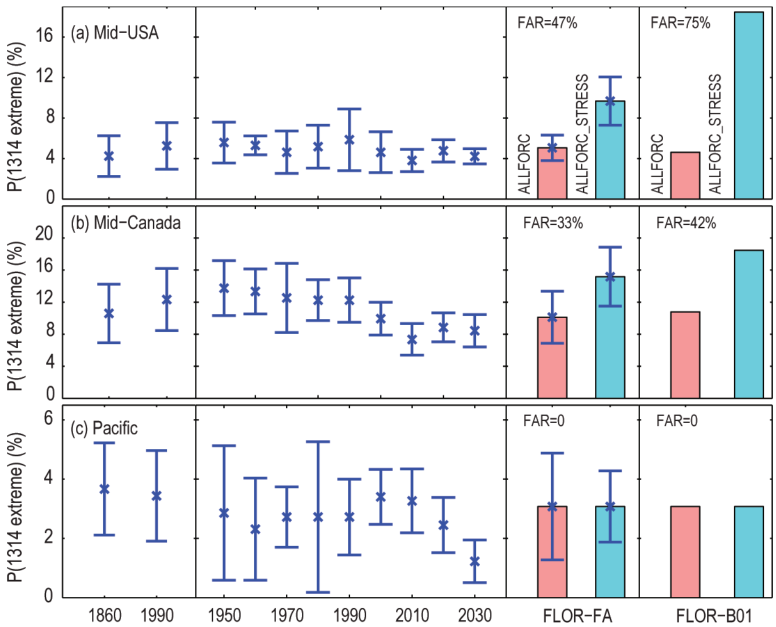

Fig. 6.2. Probability for the 2013/14 winter extreme ETSI of three regions simulated by a suite of simulations using FLOR. P(ETSI of 1314) represents the probability of occurrence of a year with ETSI more than or equal to the 2013/14 values for a given location, called the extreme probability. The error bar plots display the estimated mean P(ETSI of 1314) (cross symbols) and associated standard errors (bars). The mean and standard errors are computed from 100-year chunks from the 1990 (500 years) and 1860 (2000 years) control simulations (1st column); 100-year chunks from the 35-member historical forcing simulations every 10 years during 1941–2050 (2nd column); 91-year chunks from the 35-member ALLFORC (pink shading)/ALLFORC_STRESS (cyan shading) simulations during the hiatus period 2000–12 using FLOR_FA (3rd column). The pink (cyan) shaded bar represents the extreme probability during 2000–12 for the 5-member ALLFORC (ALLFORC_STRESS) simulations using FLOR_B01 (4th column). Fraction of attributable risk (FAR) is labelled over the shaded bars. The extreme probabilities are shown for (a) the mid-USA, (b) mid-Canada, and (c) the Pacific coastal region. The boundary of the three regions is marked in three boxes in Fig. 6.1a.

exhibit a significant decrease starting 2000 (second column of Fig. 6.2b); there is also no significant increase of the extreme occurrence over the Pacific coastal region (third column of Fig. 6.2c). Thus, the impact of anthropogenic forcing prescribed on this model did not contribute to the 2013/14 extreme ETS events over North America.

Recently, Delworth et al. (2015) found that observed multiyear changes of tropical Pacific zonal wind can drive both the global warming hiatus (consistent with Kosaka and Xie 2013; England et al. 2014) and recent multiyear western North American drying (and also an increase in precipitation in the central and eastern USA). Thus, a link may exist between the recent tropical Pacific decadal changes with the extreme ETS over North America, since the severe California drought has to be linked with reduced ETSs over California and its coastal ocean. To elucidate the possible link between the recent tropical Pacific changes and the ETS extremes over North America, we compute the extreme probabilities over the global warming hiatus period (2000–12) in an experiment with all historical radiative forcing (ALLFORC) and an experiment with radiative forcing plus observed tropical Pacific wind stress anomalies (ALLFORC_STRESS). The experiments are taken from Delworth et al. (2015), and the details can be found in SM Section 2d.

The estimated extreme probabilities from the ALLFORC_STRESS experiment during 2000–13 are significantly larger than those from the ALLFORC experiment over mid-USA and mid-Canada using FLOR_FA (third column of Figs. 6.2a and b), while the extreme probabilities are not statistically distinguishable between the two experiments over the Pacific coastal region (third column of Fig. 6.2c). The similar contrast of the extreme probability between the ALLFORC and ALLFORC_STRESS runs is reproduced using FLOR_B01 (fourth column of Fig. 6.2c). The fraction of attributable risk (FAR) of the extreme probability due to the observed zonal wind anomalies in the tropical Pacific is 47% (75%), 33% (42%) and 0% (0%) using FLOR_FA (FLOR_B01) for the mid-USA, mid-Canada, and the Pacific coast, respectively (Fig. 6.2). Thus, we conclude that the recent multiyear strengthening of the tropical Pacific easterlies increased the odds of the increase in extreme ETS occurrence probability over North America in 2013/14, but not the decrease over California.

Discussions and Conclusions. The winter of 2013/14 saw extreme ETS activity over much of North America. Based on a large ensemble of historical forcing experiments with a high-resolution coupled climate model we find no evidence to support the hypothesis that global warming contributed to this extreme ETS event. However, the recent multiyear increase in the strength of the trade winds in the tropical Pacific

Ocean that has been linked to the global warming hiatus (Kosaka and Xie 2013; England et al. 2014; Delworth et al. 2015) substantially increased the probability of the 2013/14 positive extreme ETS winter over much of North America (though it did not contribute significantly to the decrease over California). The event was unlikely even in initialized seasonal predications, highlighting the important role of stochastic forcing ("weather noise") in this event. Therefore, it is likely that the anomalous tropical Pacific Ocean state was a major climate driver of the extremely active ETSs over much of North America during the 2013/14 winter through the multiyear enhancement of the trade winds and a weak La Niña. It is likely that an enhanced probability of extreme enhanced ETS seasons like the 2013/14 winter over much of North America will continue if the anomalous easterly winds that have contributed to the global warming hiatus persist over the tropical Pacific Ocean.

ACKNOWLEDGEMENTS. This work is supported in part by NOAA's Climate Program Office. X. Yang and G. A. Vecchi are supported by NOAA/OAR under the auspices of the National Earth System Prediction Capability (National ESPC).

REFERENCES

Chang, E. K. M., 2013: CMIP5 projection of significant reduction in extratropical cyclone activity over North America. *J. Climate*, **26**, 9903–9922, doi:10.1175/JCLI-D-13-00209.1.

Dee, D. P., and Coauthors, 2011: The ERA-Interim reanalysis: Configuration and performance of the data assimilation system. *Quart. J. Roy. Meteor. Soc.*, **137**, 553–597.

Delworth, T. L., F. Zeng, A. Rosati, G. A. Vecchi, and A. T. Wittenberg, 2015: A link between the hiatus in global warming and North American drought. *J. Climate*, **28**, 3834–3845, doi:10.1175/JCLI-D-14-00616.1.

England, M. H., and Coauthors, 2014: Recent intensification of wind-driven circulation in the Pacific and the ongoing warming hiatus. *Nat. Climate Change*, **4**, 222–227, doi:10.1038/nclimate2106.

Grise, K. M., S.-W. Son, and J. R. Gyakum, 2013: Intraseasonal and interannual variability in North American storm tracks and its relationship to equatorial Pacific variability. *Mon. Wea. Rev.*, **141**, 3610–3625, doi:10.1175/MWR-D-12-00322.1.

Hartmann, D. L., 2015: Pacific sea surface temperature and the winter of 2014. *Geophys. Res. Lett.*, **42**, 1894–1902, doi:10.1002/2015GL063083.

Jia, L., and Coauthors, 2015: Improved seasonal prediction of temperature and precipitation over land in a high-resolution GFDL climate model. *J. Climate*, **28,** 2044–2062, doi:10.1175/JCLI-D-14-00112.1

Kosaka, Y., and S.-P. Xie, 2013: Recent global-warming hiatus tied to equatorial Pacific surface cooling. *Nature*, **501**, 403–407, doi:10.1038/nature12534.

Murakami, H., G. A. Vecchi, T. Delworth, K. Paffendorf, R. Gudgel, L. Jia, and F. Zeng, 2015: Investigating the influence of anthropogenic forcing and natural variability on the 2014 Hawaiian hurricane season [in "Explaining Extreme Events of 2014 from a Climate Perspective"]. *Bull. Amer. Meteor. Soc.*, **96** (12), S115-S119, doi:10.1175/BAMS-D-15-00119.1

Vecchi, G. A., and Coauthors, 2014: On the seasonal forecasting of regional tropical cyclone activity. *J. Climate*, **27**, 7994–8016, doi:10.1175/JCLI-D-14-00158.1.

Wallace, J., G. Lim, and M. Blackmon, 1988: Relationship between cyclone tracks, anticyclone tracks and baroclinic waveguides. *J. Atmos. Sci.*, **45**, 439–462.

Yang, X., and Coauthors, 2015: Seasonal predictability of extratropical storm tracks in GFDL's high-resolution climate prediction model. *J. Climate*, **28**, 3592–3611, doi:10.1175/JCLI-D-14-00517.1.

Table 34.1. ANTHROPOGENIC INFLUENCE

ON EVENT STRENGTH †			
	INCREASE	**DECREASE**	**NOT FOUND OR UNCERTAIN**
Heat	**Australia** (Ch. 31) **Europe** (Ch.13) **S. Korea** (Ch. 19)		**Australia, Adelaide & Melbourne** (Ch. 29) **Australia, Brisbane** (Ch.28)
Cold		**Upper Midwest** (Ch.3)	
Winter Storms and Snow			**Eastern U.S.** (Ch. 4) **N. America** (Ch. 6) **N. Atlantic** (Ch. 7)
Heavy Precipitation	**Canada**** (Ch. 5)		**Jakarta****** (Ch. 26) **United Kingdom***** (Ch. 10) **New Zealand** (Ch. 27)
Drought	**E. Africa** (Ch. 16) **E. Africa*** (Ch. 17) **S. Levant** (Ch. 14)		**Middle East and S.W. Asia** (Ch. 15) **N.E. Asia** (Ch. 21) **Singapore** (Ch. 25)
Tropical Cyclones			**Gonzalo** (Ch. 11) **W. Pacific** (Ch. 24)
Wildfires			**California** (Ch. 2)
Sea Surface Temperature	**W. Tropical & N.E. Pacific** (Ch. 20) **N.W. Atlantic & N.E. Pacific** (Ch. 13)		
Sea Level Pressure	**S. Australia** (Ch. 32)		
Sea Ice Extent			**Antarctica** (Ch. 33)

† Papers that did not investigate strength are not listed.

†† Papers that did not investigate likelihood are not listed.

* No influence on the likelihood of low rainfall, but human influences did result in higher temperatures and increased net incoming radiation at the surface over the region most affected by the drought.

** An increase in spring rainfall as well as extensive artificial pond drainage increased the risk of more frequent severe floods from the enhanced rainfall.

*** Evidence for human influence was found for greater risk of UK extreme rainfall during winter 2013/14 with time scales of 10 days

**** The study of Jakarta rainfall event of 2014 found a statistically significant increase in the probability of such rains over the last 115 years, though the study did not establish a cause.

	ON EVENT LIKELIHOOD ††			Total Number of Papers
	INCREASE	DECREASE	NOT FOUND OR UNCERTAIN	
Heat	**Argentina** (Ch. 9) **Australia** (Ch. 30, Ch. 31) **Australia, Adelaide** (Ch. 29) **Australia, Brisbane** (Ch. 28) **Europe** (Ch. 13) **S. Korea** (Ch. 19) **China** (Ch. 22)		**Melbourne, Australia** (Ch. 29)	7
Cold		**Upper Midwest** (Ch.3)		1
Winter Storms and Snow	**Nepal** (Ch. 18)		**Eastern U.S.**(Ch. 4) **N. America** (Ch. 6) **N. Atlantic** (Ch. 7)	4
Heavy Precipitation	**Canada**** (Ch. 5) **New Zealand** (Ch. 27)		**Jakarta****** (Ch. 26) **United Kingdom***** (Ch. 10) **S. France** (Ch. 12)	5
Drought	**E. Africa** (Ch. 16) **S. Levant** (Ch. 14)		**Middle East and S.W. Asia** (Ch. 15) **E. Africa*** (Ch. 17) **N.E. Asia** (Ch. 21) **S. E. Brazil** (Ch. 8) **Singapore** (Ch. 25)	7
Tropical Cyclones	**Hawaii** (Ch. 23)		**Gonzalo** (Ch. 11) **W. Pacific** (Ch. 24)	3
Wildfires	**California** (Ch. 2)			1
Sea Surface Temperature	**W. Tropical & N.E. Pacific** (Ch. 20) **N.W. Atlantic & N.E. Pacific** (Ch. 13)			2
Sea Level Pressure	**S. Australia** (Ch. 32)			1
Sea Ice Extent			**Antarctica** (Ch. 33)	1
			TOTAL	**32**

† Papers that did not investigate strength are not listed.

†† Papers that did not investigate likelihood are not listed.

* No influence on the likelihood of low rainfall, but human influences did result in higher temperatures and increased net incoming radiation at the surface over the region most affected by the drought.

** An increase in spring rainfall as well as extensive artificial pond drainage increased the risk of more frequent severe floods from the enhanced rainfall.

*** Evidence for human influence was found for greater risk of UK extreme rainfall during winter 2013/14 with time scales of 10 days

**** The study of Jakarta rainfall event of 2014 found a statistically significant increase in the probability of such rains over the last 115 years, though the study did not establish a cause.